Communication

# Metalation of a Mesoporous Three-Dimensional Covalent Organic Framework

Luke A. Baldwin, Jonathan W. Crowe, David A. Pyles, and Psaras L. McGrier

*J. Am. Chem. Soc.*, **Just Accepted Manuscript** • DOI: 10.1021/jacs.6b10316 • Publication Date (Web): 04 Nov 2016

# Metalation of a Mesoporous Three-Dimensional Covalent Organic Framework

Luke A. Baldwin, Jonathan W. Crowe, David A. Pyles, Psaras L. McGrier*

Department of Chemistry and Biochemistry, The Ohio State University, Columbus, Ohio, 43210, United States

*Supporting Information Placeholder*

**ABSTRACT** Constructing metalated three-dimensional (3D) covalent organic frameworks is a challenging synthetic task. Herein, we report the synthesis and characterization of a highly porous ($SA_{BET}$ = 5083 $m^2$ $g^{-1}$) 3D COF with a record low density (0.13 g $cm^{-3}$) containing π-electron conjugated dehydrobenzoannulene (DBA) units. Metalation of DBA-3D-COF 1 with Ni to produce Ni-DBA-3D-COF results in a minimal reduction in the surface area ($SA_{BET}$ = 4763 $m^2$ $g^{-1}$) of the material due to the incorporation of the metal within the cavity of the DBA units, and retention of crystallinity. Both 3D DBA-COFs also display great uptake capacities for ethane and ethylene gas.

Covalent organic frameworks (COFs)[1-4] are an exceptional class of porous crystalline materials that possess low densities, great thermal stabilities, and high internal surface areas. Over the past decade, these characteristics have made COFs attractive candidates for applications related to gas storage,[5,6] separations,[7,8] optoelectronics,[9-13] catalysis,[14,15] and energy storage.[16,17] The modular nature of COFs provides a unique platform to incorporate various rigid molecular building blocks that can be metalated to enhance their catalytic[18] and gas adsorption properties.[19,20,21] While the construction of two-dimensional (2D) COFs containing metalated porphyrin,[22] phthalocyanine,[23] and bipyridine[24] units have become fairly prevalent, finding efficient ways to synthesize novel three-dimensional (3D)[25-28] COFs that can be metalated without compromising the surface area or pore volume of the material is still a challenge. As a consequence, only one metalated 3D COF has been reported.[29] The limited number of metalated 3D COFs is likely attributed to the synthetic challenge of utilizing the right geometrically shaped monomers that can not only produce crystalline polymeric networks but also form strong complexes with metal ions. Finding monomers that can accomplish this task would be essential for constructing lightweight crystalline materials that could potentially rival their metal-organic framework (MOF)[30] counterparts.

Herein, we present the synthesis and metalation of a mesoporous 3D COF containing $C_3$-symmetric π-electron conjugated dehydrobenzoannulene (DBA)[31] and tetrahedral *tetra*(4-dihydroxyborylphenyl)methane (TBPM) units. DBAs are planar triangular shaped macrocycles that are capable of forming strong metal complexes with Li,[32] and Ca,[33] and low oxidation state transition metals.[34,] The planarity and metal binding properties of DBAs are comparable to porphyrin and phthalocyanine ligands, which typically use hard nitrogen atoms to bind metals. In contrast, DBAs are neutral compounds that contain soft ligands capable of donating 2-4 electrons per alkyne depending on the electronic demands of the metals.[35] We demonstrate that DBA[12] and TBPM monomers can be utilized to form a crystalline 3D polymer network with the lowest density (0.13 g $cm^{-3}$) and highest BET surface area (5083 $m^2$ $g^{-1}$) reported to date for a COF. We also show that the metalation of DBA-3D-COF 1 with $Ni(COD)_2$ to obtain Ni-DBA-3D-COF results in a minimal reduction in the pore volume and surface area of the material. Interestingly, both materials display great uptake capacities for ethane and ethylene gas.

**Scheme 1. Synthesis of DBA-3D-COF 1 Using TBPM and DBA[12] Units Followed by Metalation with $Ni(COD)_2$ to Produce Ni-DBA-3D-COF.**

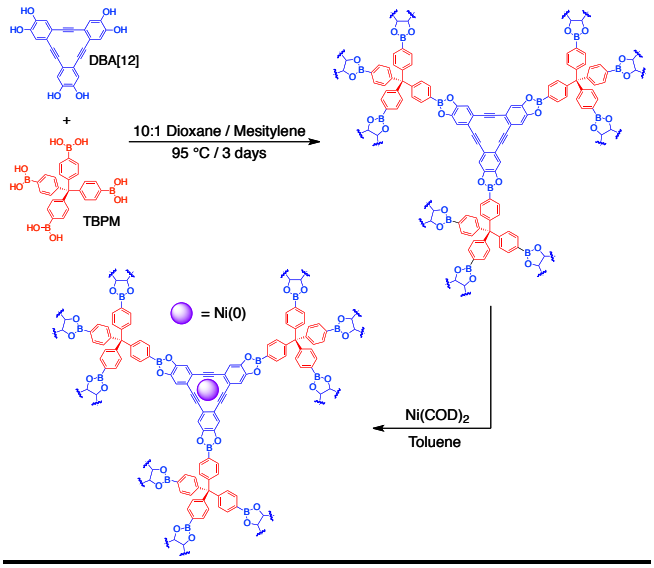


DBA-3D-COF 1 was synthesized under solvothermal conditions by reacting DBA[12] with TBPM in a 10:1 (v/v) 1,4-dioxane and mesitylene mixture in flame-sealed glass ampules at 95°C for 3 days (Scheme 1). DBA-3D-COF 1 was obtained by filtration and washed with acetonitrile in an argon-purged

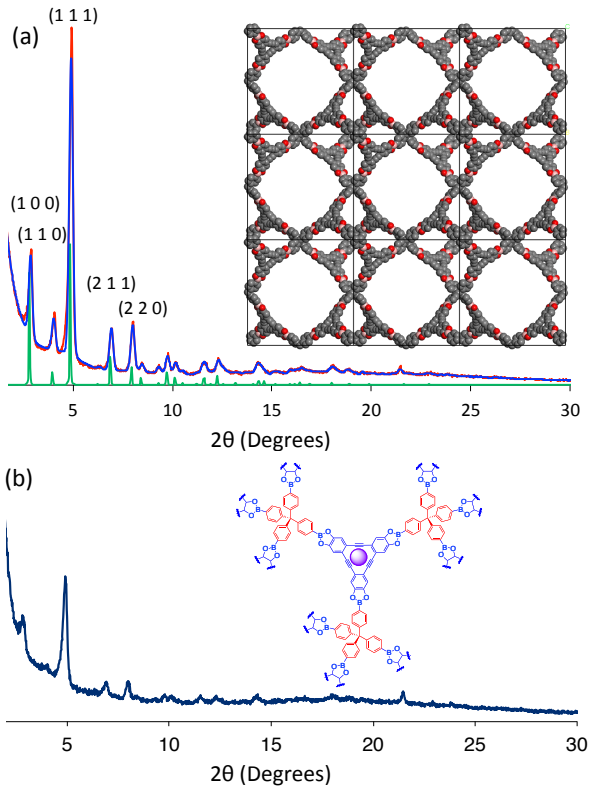


**Figure 1.** (a) Indexed experimental (red) and Pawley refined (blue) PXRD patterns of DBA-3D-COF 1 compared to the **bor** simulated unit cell (green) with views along the x and y direction of the cubic crystal model. (b) PXRD of Ni-DBA-3D-COF with a structure showing Ni(0) (purple circle) bound in the cavity of DBA[12].

glove box to produce a light green crystalline powder. The ideal reaction conditions were obtained by screening different temperatures, monomer and solvent ratios, and reaction times. (see pp. S10 in the Supporting information (SI)). It should be noted that samples in which both DBA[12] and TBPM monomers were fully soluble prior to sealing the ampules typically yielded the best results. These homogeneous conditions are consistent with what has been observed for obtaining the efficient growth of 2D COFs.[36] Thermogravimetric analysis revealed that DBA-3D-COF 1 maintains ~ 95% of it's weight up to 458°C (Figure S13, SI). Scanning electron microscopy (SEM) images revealed the formation of rhombic shaped crystallites (Figure S26, SI). Metalation was achieved by adding a solution containing 10 wt% $Ni(COD)_2$ dissolved in 1 mL of dry toluene to ~34 mg of DBA-3D-COF 1. The mixture was then stirred at room temperature in an argon-purged glove box for 24 h to produce Ni-DBA-3D-COF as a dark purple crystalline powder. Ni-DBA-3D-COF was obtained by filtration, washed with dry toluene to remove excess $Ni(COD)_2$, and dried under vacuum at 35°C for 16 h.

The crystallinity of DBA-3D-COF 1 and Ni-DBA-3D-COF were evaluated using powder X-ray diffraction (PXRD). Figure 1a shows the experimental and refined PXRD profile for DBA-3D-COF 1. Since DBA-3D-COF 1 was constructed utilizing tetrahedral and triangular shaped monomers, we predicted that combining both structures would yield a non-interpenetrated 3D cubic lattice with a **bor** (*P*-43*m*) net topology reminiscent of COF-108.[24] DBA-3D-COF 1 exhibited intense peaks at 2.88, 4.01, 4.92, 6.89, 7.97°, which correspond to the (100), (110), (111), (211), and (220) planes respectively. The crystal structure of DBA-3D-COF 1 was simulated using the Reflex module of the Materials Studio 7.0 software. Pawley refinement of the experimental data using a **bor** net provided unit cell parameters of a = b = c = 31.953 Å (residuals $R_p$= 6.44, $R_{wp}$= 9.70). The simulated PXRD profile was in good agreement with the experimental data. We also considered the **ctn** net, but the simulated PXRD did not match the experimental data (Figure S6, SI). In addition, DBA-3D-COF 1 exhibits a density of 0.13 g $cm^{-3}$, which is lower than the reported densities of COF-102 (0.41 g $cm^{-3}$), COF-105 (0.18 g $cm^{-3}$), and COF-108 (0.17 g $cm^{-3}$). The PXRD profile of Ni-DBA-3D-COF revealed retention of crystallinity and preservation of the framework following metalation with $Ni(COD)_2$ (Figure 1b). Interestingly, Fourier transform infrared (FT-IR) spectroscopy revealed similar B-O stretching modes at 1340 and 1337 $cm^{-1}$ for DBA-3D-COF 1 and Ni-DBA-3D-COF, respectively (Figures S1 & S2, SI). This suggests that the metal is bound exclusively in the cavity of DBA[12] to produce a Ni(0) complex[37] with no interaction at the boronate ester linkage. Inductively coupled plasma-atomic emission spectroscopy (ICP-AES) analysis indicated that ~10.1 wt% of Ni was incorporated into Ni-DBA-3D-COF.

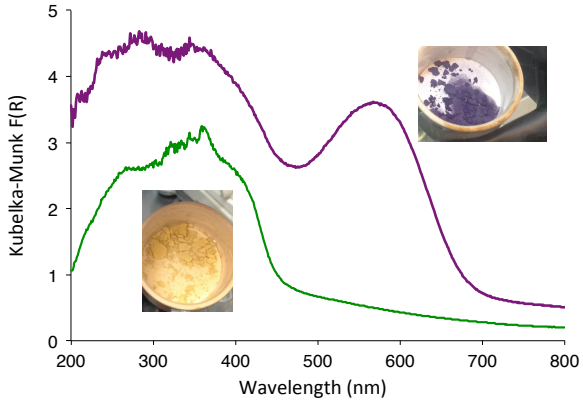


**Figure 2.** Kubelka-Munk diffuse reflectance spectra and photographs of DBA-3D-COF 1 (green) and Ni-DBA-3D-COF (purple).

In order to confirm the presence of DBA-Ni(0) complex, we also characterized DBA-3D-COF 1 and Ni-DBA-3D-COF utilizing solid-state $^{13}C$ cross-polarization magic angle spinning (CP-MAS) NMR, UV-vis diffuse reflectance, and solid-state fluorescence spectroscopies. The presence of the alkynyl units for DBA-3D-COF 1 were confirmed by $^{13}C$ CP-MAS NMR exhibiting a distinct resonance at ~ 91 ppm (Figure S7, SI). Upon metalation, the alkynyl peak of DBA-3D-COF 1 experienced 15 ppm downfield shift from 91 to 106 ppm due to the formation of a DBA-Ni(0) complex (Figure S8, SI.) These results are consistent with $^{13}C$ NMR shifts that were previously reported by Youngs and coworkers for a single molecule DBA-Ni(0) complex.[37] The UV-vis diffuse-reflectance spectrum of DBA-3D-COF 1 exhibits a broad absorbance from 300 to 420 nm (Figure 2). After metalation, a new charge transfer absorption band emerges at ~ 575 nm for Ni-DBA-3D-COF, which is indicative of three alkynyl units donating 2e- to form the

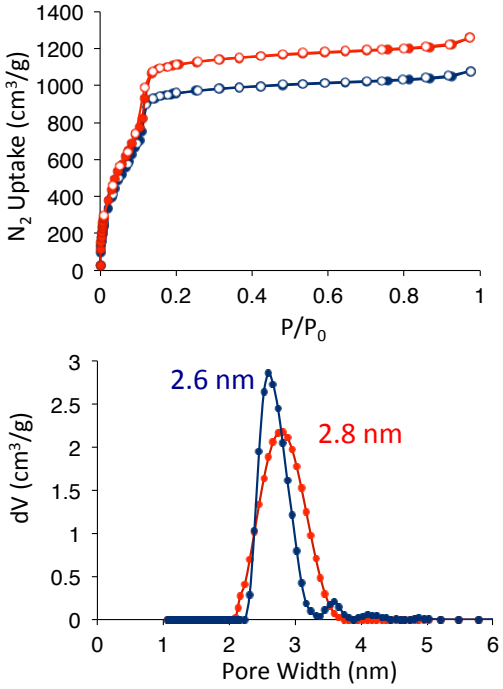


**Figure 3.** Nitrogen adsorption/desorption isotherms (top) and NLDFT pore size distributions (bottom) for DBA-3D-COF 1 (red) and Ni-DBA-3D-COF (blue) measured at 77 K.

DBA-Ni(0) 16 electron complex. In addition, DBA-3D-COF 1 is highly luminescent in the solid-state exhibiting a $\lambda_{max}$ of 510 nm, which is blue-shifted by ~ 20 nm from the 2D DBA-COFs[38,39] (Figure S27, SI). However, the luminescence of DBA-3D-COF 1 is quenched after metalation further indicating that the Ni(0) is being incorporated within the triangular pore of the DBA[12] units.

X-ray photoelectron spectroscopy (XPS) analysis of $Ni(COD)_2$ and Ni-DBA-3D-COF revealed the presence of two Ni species with different oxidation states (Figure S29, SI). $Ni(COD)_2$ displayed two broad peaks at 856.26 and 853.26 eV, which correspond to the core energy levels of Ni(II)$2p_{3/2}$ and Ni(0) $2p_{3/2}$, respectively. In contrast, the energy level for Ni(0) $2p_{3/2}$ shifts upfield by ~ 0.8 eV to 852.44 eV for Ni-DBA-3D-COF indicating that the Ni(0) atoms are binding with the alkynyl units of DBA[12]. The broad peak for the Ni(II)$2p_{3/2}$ energy level of Ni-DBA-3D-COF experienced a small upfield shift of ~ 0.1 eV which suggests a weak binding interaction with the alkynyl units. The presence of the boron, carbon, and oxygen atoms of Ni-DBA-3D-COF were also confirmed by XPS (Figure S28, SI).

The porosity of DBA-3D-COF 1 and Ni-DBA-3D-COF were determined by nitrogen gas adsorption measurements at 77 K. DBA-3D-COF 1 exhibited a type-IV isotherm displaying a sharp uptake at low relative pressure ($P/P_0 < 0.1$) followed by a sharp step between $P/P_0 = 0.05$ and 0.13 which is indicative of a mesoporous material (Figure 3), The Brunauer-Emmet-Teller (BET) model was applied over the low-pressure region ($0.07 < P/P_0 < 0.11$) of the isotherm to provide a surface area of 5083 $m^2 g^{-1}$. It should be noted that the BET surface area of DBA-3D-COF 1 is larger than COF-102 (3472 $m^2 g^{-1}$) and COF-103 (4210 $m^2 g^{-1}$).[24] The pore size distribution of DBA-3D-COF 1, which was estimated using nonlocal density functional theory (NLDFT), provided an average pore size of 2.8 nm. The experimental pore size is close to the predicted value of 3.1 nm. The total pore volume calculated at $P/P_0 = 0.974$ afforded a value of 1.85 $cm^3 g^{-1}$. Surprisingly, Ni-DBA-3D-COF also exhibited a type-IV isotherm. Application of the BET model over the low-pressure $0.07 < P/P_0 < 0.11$ range provided a surface area of 4763 $m^2 g^{-1}$. The NLDFT pore size of Ni-DBA-3D-COF experienced a slight 0.2 nm decrease to provide an average pore size of 2.6 nm. The total pore volume calculated at $P/P_0 = 0.975$ yielded a value of 1.59 $cm^3 g^{-1}$. Since we believe Ni(0) is predominantly bound within the triangular pore of the DBA[12] units, we believe that these slight reductions are likely attributed to small a quantity of unbound Ni(II) trapped within the pores of the material.

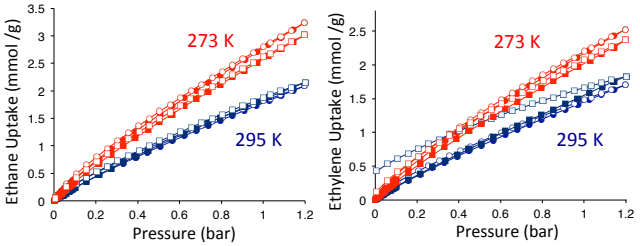


**Figure 4.** Ethane (left) and ethylene (right) adsorption/desorption isotherms for DBA-3D-COF 1 (circle) and Ni-DBA-3D-COF (square). All isotherms were measured at 273 K (red) and 295 K (blue).

To determine if Ni-DBA-3D-COF could be effective at performing ethane/ethylene separations, we measured gas adsorption isotherms for both COFs at 273 and 295 K from 0 to 1.2 bar (Figure 4). DBA-3D-COF 1 exhibited swift uptake of ethane at low pressures reaching capacities of 3.24 mmol $g^{-1}$ at 273 K and 2.09 mmol $g^{-1}$ at 295 K. The ethylene uptake capacities were much lower reaching values of 2.52 mmol $g^{-1}$ at 273 K and 1.70 mmol $g^{-1}$ at 295 K. In comparison, Ni-DBA-3D-COF displayed uptake capacities of 3.01 mmol $g^{-1}$ and 2.16 mmol $g^{-1}$ for ethane, and 2.36 mmol $g^{-1}$ and 1.83 mmol $g^{-1}$ for ethylene at 273 and 295 K, respectively. Surprisingly, the metalated Ni-DBA-3D-COF displayed only a modest increase of 0.07 mmol for ethane, and 0.13 mmol for ethylene at 295 K. These slight increases are likely attributed to the ability of the open Ni(0) sites to polarize ethane,[40] and weak π - complexation between the d-orbitals of Ni(0) and the π orbitals of ethylene.[41] The ethane/ethylene selectivities of DBA-3D-COF 1 and Ni-DBA-3D-COF were calculated using initial slope calculations in the pressure range of 0-0.1 bar to afford values of 1.25 and 1.28 at 273 K, and 1.24 and 1.15 at 295 K, respectively (Figures S16-S19, SI). The isosteric heats of adsorption ($Q_{st}$) were estimated using the virial method to assess the binding affinity of ethane and ethylene to both materials. DBA-3D-COF 1 exhibited $Q_{st}$ values of 16.8 kJ $mol^{-1}$ for ethane and 15.9 kJ $mol^{-1}$ ethylene, while Ni-DBA-3D-COF displayed $Q_{st}$ values of 11.6 kJ $mol^{-1}$ for ethane and 9.7 kJ $mol^{-1}$ for ethylene at 295 K, at zero coverage (Figures S20 & S21, SI). These results indicate that the open metal sites of Ni-DBA-3D-COF do not significantly enhance their binding interactions with ethane or ethylene relative to DBA-3D-COF 1. However, Ni-DBA-3D-COF could be useful as a neutral heterogeneous catalyst for ethylene polymerizations.[42]

In conclusion, we have demonstrated that a DBA[12] monomer can be used to create a highly porous 3D COF that retains its crystallinity upon metalation with Ni. Metalation of

DBA-3D-COF 1 results in a minimal reduction in the surface area and pore volume of the material. To the best of our knowledge, this is the first example of metalating a 3D COF with Ni. The proof-of-principle is important, as DBA monomers also have the ability to bind Li,[32] Ca,[33] and other low oxidation state transition metals.[34,35] With this in mind, we believe this work increases the prospect of using metalated DBA-based COFs for applications related to catalysis,[43] gas storage,[19-21] spintronics,[44] and separations.[45]

ASSOCIATED CONTENT

## Supporting Information

Synthetic procedures, FT-IR, solid-state $^{13}C$ NMR, XPS, TGA PXRD, and SEM. This material is available free of charge via the internet at http://pubs.acs.org.

The Supporting Information is available free of charge on the ACS Publications website.

## AUTHOR INFORMATION

### Corresponding Author

*mcgrier.1@osu.edu

### Notes

The authors declare no competing financial interests.

## ACKNOWLEDGMENTS

P.L.M acknowledges the National Science Foundation (NSF) and Georgia Tech Facilitating Academic Careers in Engineering and Science (GT-FACES) for a Career Initiation Grant, and funding from The American Chemical Society Petroleum Research Fund (55562-DNI7), NSF (DMR-0114098), and The Ohio State University.

## REFERENCES

(1) a.) Côté, A.P.; Benin, A.I; Ockwig, N.W; O'Keeffe, M.; Matzger, A.J.; Yaghi, O. M. *Science* **2005**, *310*, 1166-1170. b.) Waller, P. J.; Gándara, F.; Yaghi, O. M. *Acc. Chem. Res.* **2015**, *48*, 3053-3063.

(2) Tilford, R. W.; Gemmil, W. R.; zur Loye, H.-C.; Lavigne, J. J. *Chem. Mater.* **2006**, *18*, 5296-5301.

(3) Ding, S.-Y.; Wang, W. *Chem. Soc. Rev.* **2012**, *42*, 548-568.

(4) Huang, N.; Wang, P.; Jiang, D. *Nat. Rev. Mater.* **2016**, *1*, 16068-16086.

(5) Furukawa, H.; Yaghi, O. M. *J. Am. Chem. Soc.* **2009**, *131*, 8875-8883.

(6) Zeng, Y.; Zou, R.; Zhao, Y. *Adv. Mater.* **2016**, 28, 2855-2873

(7) Oh, H.; Kalidini, S.B; Um, Y; Bureekaew, S.; Schmid, R.; Fischer, R.A.; Hirsher, M. *Angew. Chem. Int. Ed.*, **2013**, *52*, 13219-13222.

(8) Kang, Z.; Peng, Y.; Qian, Y.; Yuan, D.; Addicoat, M. A.; Heine, T.; Hu, Z.; Tee, L.; Guo, Z.; Zhao, D. *Chem. Mater.* **2016**, *28*, 1277-1285.

(9) Wan, S.; Guo, J.; Kim, J.; Ihee, H; Jiang, D. *Angew. Chem., Int. Ed.* **2008**, *47*, 8826-8830.

(10) Spitler, E. L.; Dichtel, W. R. *Nat. Chem.* **2010**, *2*, 672-677.

(11) Bertrand, G. H. V.; Michaelis, V. K.; Ong, T.-C.; Griffin, R. G.; Dincă, M. *Proc. Natl. Acad. Sci U. S. A.* **2013**, *110*, 4923-4928.

(12) Dogru, M.; Handloser, M.; Auras, F.; Kunz T.; Medina, D.; Hartschuh, A.; Knochel, P; Bein T. A. *Angew. Chem., Int. Ed.* **2013**, *52*, 2920-2924.

(13) Duhović, S.; Dincă, M. *Chem. Mater.* **2016**, *28*, 2855-2873.

(14) Ding, S.-Y.; Gao, J.; Wang, Q; Zhang, Y.; Song, W.-G.; Su, C.-Y.; Wang, W. *J. Am. Chem. Soc.* **2011**, *133*, 19816-19822.

(15) Fang, Q.; Gu, S.; Zheng, J.; Zhuang, Z.; Qiu, S; Yan, Y. *Angew. Chem., Int. Ed.* **2014**, *53*, 2878-2882.

(16) Deblase, C. R.; Silberstein, K. E.; Truong, T.-T.; Abruña, H. D.; Dichtel, W. R. *J. Am. Chem. Soc.* **2014**, *135*, 16821-16824.

(17) Mulzer, C.; Shen, L.; Bisbey, R. P.; McKone, J. R.; Zhang, N.; Abruña, H. D.; Dichtel, W. R. *ACS Cent. Sci.* **2016**, *2*, 667-673.

(18) Pachfule, P.; Kandambeth, S.; Diaz Diaz. D.; Banerjee, R. *Chem. Commum.* **2014**, *50*, 3169-3172.

(19) Cao, D.; Lan, J.; Wang, W.; Smit, B. *Angew. Chem. Int. Ed.* **2009**, *48*, 4730–4733.

(20) Lan, J.; Cao, D.; Wang, W.; Smit, B. *ACS Nano* **2010**, *4*, 4225-4237.

(21) Mendoza-Cortes, J. L.; Goddard, W. A.; Furukawa, H.; Yaghi, O. M. *J. Phys. Chem. Lett.* **2012**, *3*, 2671-2675.

(22) Lin, S.; Diercks, C. S.; Zhang, Y.-B.; Kornienko, N.; Nichols, E. M.; Zhao, Y.; Paris, A. R.; Kim, D.; Yang, P.; Yaghi, O. M.; Chang, C. J. *Science* **2016**, *349*, 1208-1213.

(23) Spitler, E. L.; Colson, J. W.; Uribe-Romo, F. J.; Woll, A. R.; Giovino, M. R.; Saldivar, A.; Dichtel, W. R. *Angew. Chem. Int. Ed.* **2012**, *51*, 2623-2627.

(24) Aiyappa, H. B.; Thote, J.; Shinde, D. B.; Banerjee, R.; Kurungot, S. *Chem. Mater.* **2016**, *28*, 4375-4379.

(25) El-Kaderi, H. M.; Hunt, J.R.; Mendoza-Cortes, J. L.; Côté, A.P.; Taylor, R. E.; O'Keeffe, M. O.; Yaghi, O. M. *Science* **2007**, *316*, 268-272.

(26) Uribe-Romo, F. J.; Hunt, J. R.; Furukawa, H.; Klöck, C.; O'Keeffe, M.; Yaghi, O. M. *J. Am. Chem. Soc.* **2009**, *131*, 4570–4571.

(27) Bunck, D. N.; Dichtel, W. R. *Angew. Chem. Int. Ed.* **2012**, *51*, 1885–1889.

(28) Lin, G.; Ding, H.; Yuan, D.; Wang, B.; Wang, C. *J. Am. Chem. Soc.* **2016**, *138*, 3302–3305.

(29) Liu, Y.; Ma,Y.; Zhao, Y.; Sun, X.; Gandara, F.; Furukawa, H.; Liu, Z.; Zhu, H.; Zhu, C.; Suenaga, K.; Oleynikov, P.; Alshammari, A. S.; Zhang, X.; Teraskai, O.; Yaghi, O. M. *Science* **2016**, *351*, 365-369.

(30) Evans, J. D.; Sumby, C. J.; Doonan, C. J. *Chem. Soc. Rev.* **2014**, *43*, 5933-5951.

(31) Spitler, E. L.; Johnson II, C. A.; Haley, M. M. *Chem Rev.* **2006**, *106*, 5344-5386.

(32) Zhang, H.; Zhao, M.; He, X.; Wang, Z.; Zhang, X.; Liu, X. *J. Phys. Chem. C.* **2011**, *115*, 8845-8850.

(33) Li, C.; Li, J.; Wu, F.; Li, S.-S.; Xia, J.-B.; Wang, L.-W. *J. Phys. Chem. C.* **2011**, *115*, 23221-23225.

(34) Srinivasu, K.; Ghosh, S. K. *J. Phys. Chem. C.* **2013**, *117*, 26021-26028.

(35) Youngs, W. J.; Tessier, C. A.; Bradshaw, J. D. *Chem. Rev.* **1999**, *99*, 3153-3180.

(36) Smith, B.J.; Dichtel, W. R. *J. Am. Chem. Soc.* **2014**, *136*, 8783-8789.

(37) Ferrara, J. D..; Tessier-Youngs, C.; Youngs, W. J. *J. Am. Chem. Soc.* **1985**, *107*, 6719-6721.

(38) Baldwin, L. A.; Crowe, J. W.; Shannon, M. D.; Jaroniec, C. P.; McGrier, P. L. *Chem. Mater.* **2015**, *27*, 6169-6172.

(39) Crowe, J. W.; Baldwin, L. A., McGrier, P. L. *J. Am. Chem. Soc.* **2016**, *138*, 10120-10123.

(40) Liang, W.; Xu, F.; Zhou, X.; Xiao, J.; Xia, Q.; Li, Y.; Li, Z. *Chem. Eng. Sci.* **2016**, *148*, 275-281.

(41) Safarik, D.J.; Eldridge, R.B. *Ind. Eng. Chem Res.* **1998**, *37*, 2571.

(42) Gao, R.; Sun, W.-H.; Redshaw, C. *Catal. Sci. Technol.* **2013**, *3*, 1172-1179.

(43) Tanabe, K. K.; Ferrandon, M.S.; Siladke, N. A.; Kraft, S. J.; Zhang, G.; Niklas, J.; Poluektov, O. G.; Lopykinski, S. J.; Bunel, E. E.; Krause, T. R.; Miller, J. T.; Hock, A. S.; Nguyen, S. T. *Angew. Chem., Int. Ed.* **2014**, *53*, 12055-12058

(44) He, J.; Ma, S. Y.; Zhou, P.; Zhang, C. X.; He, C.; Sun, L. Z. *J. Phys. Chem. C.* **2012**, *116*, 26313-26321.

(45) Li, B.; Zhang, Y.; Krishna, R.; Yao, K.; Han, Yu, H.; Wu, Z.; Ma, D.; Shi, Z.; Pham, T.; Space, B.; Liu, J.; Thallapally, P. K.; Liu, J.; Chrzanowski, Ma, S. *J. Am. Chem. Soc.* **2014**, *136*, 8654-8660.

TOC